Organic Electronics 41 (2017) 280–286

Contents lists available at ScienceDirect

Organic Electronics

journal homepage: www.elsevier.com/locate/orgel

Efficient light trapping and interface engineering for performance enhancement in PTB7-Th: $PC_{70}BM$ organic solar cells

Kunal Borse [1], Ramakant Sharma [1], H.P. Sagar, P. Anil Reddy, Dipti Gupta*, Aswani Yella*

Department of Metallurgical Engineering and Material Science, Indian Institute of Technology Bombay, Powai, Mumbai, 400076, India

ARTICLE INFO

Article history:
Received 18 October 2016
Received in revised form
4 November 2016
Accepted 11 November 2016
Available online 18 November 2016

Keywords:
Organic solar cells
PTB7-Th
$PC_{70}BM$
Interface engineering
Efficient light trapping
PDMS texturing

ABSTRACT

Inefficient light absorption and poor charge separation are considered as two major bottlenecks for achieving highly efficient bulk heterojunction organic solar cells (BHJ OSCs). In the present study, we have introduced an additional phenyl-C71-butyric acid methyl ester ($PC_{70}BM$) layer to modify the interface between ZnO based electron transport layer (ETL) and photoactive layer comprised of Poly[4,8-bis(5-(2-ethylhexyl)thiophen-2-yl)benzo[1,2-b; 4,5-b′]dithiophene-2,6-diyl-alt-(4-(2-ethylhexyl)-3-fluorothieno[3,4-*b*]thio-phene-)-2-carb-oxylate-2-6-diyl)] (PTB7-Th):$PC_{70}BM$. This interface engineering has quenched the electron–hole recombination at the interface and has improved power conversion efficiency (PCE) from 6.65 to 7.74%. Devices were fabricated in an inverted geometry having a structure ITO/ZnO (40 nm)/$PC_{70}BM$ (5 nm)/PTB7-Th:$PC_{70}BM$ (70 nm)/MoO_3 (10 nm)/Ag (100 nm). Additionally, V-grooved textured PDMS films were attached to the backside of OSC substrates which has further improved PCE to 9.12%. Our study suggests that the performance enhancement as observed in OSCs with V-grooved textured PDMS films could be due to increased total optical path length of the incident light within the device.

1. Introduction

Solution processed bulk heterojunction organic solar cells (OSCs) offers many advantages such as good cost-efficiency balance, short energy payback time and unique form-factor and therefore have attracted a significant attention in recent years [1–5]. However, their power conversion efficiency (PCE) is way behind the other emerging PV technologies [6,7]. To improve the device performance, researchers have adopted two different strategies: (i) to design and develop new donor and/or acceptor molecules and (ii) to optimize various aspects of device engineering processes [8–12]. Both these strategies aims at overcoming the two major impediments restricting the PCE i.e. inefficient light absorption of the donor molecules and inefficient charge collection at the interface at donor/acceptor and/or active layer and transport layer. Over the years, it has been demonstrated that the PCE can be improved by designing new donor polymers from ~3% with poly(3-hexylthiophene) (P3HT): phenyl-C71-butyric acid methyl ester ($PC_{70}BM$) OSCs to over 10%with Poly[(5,6-difluoro-2,1,3-benzothiadiazol-4,7-diyl)-*alt*-(3,3‴-di(2-octyldodecyl)-2,2′; 5′,2″; 5″,2‴-quaterthiophen-5,5‴-diyl)](PffBT4T-2OD):$PC_{70}BM$ OSCs [11–15]. These recent low bandgap donor molecules have not only shown improved photons harvesting over the wide spectral range but also have demonstrated improved charge mobility as compared to the previously reported donor molecules [11,12]. Thus, a substantial increase in PCE can be achieved by designing and developing new low bandgap donor molecules. However, in the last two decades a very handful of donor molecule seems to be promising and thus making the choices limited [11–13,15,16]. To improve the PCE further by 10–20% of the reference devices using the known donor polymers with the marginal increase in the cost of OSCs, optimization of various aspects of device engineering processes needs to be thought of.

Some of the approaches of device engineering involve use of different combinations of electron and/or hole transport layers, solvent additives, incorporation of metal, dielectric and/or semiconducting nanoparticles (NPs), etc. [17–22]. These modifications have been proved beneficial to enhance the device performance. However, this increase in PCE is limited due to various factors such as poor quality of interface between ETL/HTL and active layer, alteration in the active layer morphology due to incorporation of metal, dielectric and/or semiconducting nanoparticles (NPs). The

* Corresponding authors.
E-mail addresses: diptig@iitb.ac.in (D. Gupta), aswani.yella@iitb.ac.in (A. Yella).
[1] Kunal Borse and Ramakant Sharma contributed equally to this work.

http://dx.doi.org/10.1016/j.orgel.2016.11.016
1566-1199/

problem of the poor quality of the interface between ETL/HTL and active layer is not that complicated and can be addressed by introducing the interlayer so as to achieve smooth interface [23–25]. But problem of alteration in the active layer morphology due to incorporation of metal, dielectric and/or semiconducting nanoparticles (NPs) and SWCNTs in some cases is somewhat critical. On the one hand introduction of various nanoparticles (NPs) facilitates the trapping of light due to enhanced optical path length [26,27]. In particular, when metal NPs are introduced in active layer, they can additionally offer local surface plasmon resonance, therefore, when an incident light with a similar mode of frequency interacts with the NPs, its energy can be stored in the oscillation mode of the NPs resulting in more absorption and/or scattering [18]. However, most of these NPs are generally synthesized using the chemical routes and have lot of surface defects which acts as a trap centres. Further, if their concentration is increased beyond the optimized concentration, they will occupy more volume fraction of active layer and therefore the probability of scattered photon getting absorbed again gets decreased [19,20]. Both these issues related to incorporation of NPs restrict the improvement in performance. Thus, it is necessary to employ non-destructive efficient light trapping technique which will not alter or modify the active layer and will not have trap centres. Various light trapping techniques were previously used to improve the performance of OSCs. These include use of textured substrates, micro-prisms, diffraction gratings, stress-induced micro-scale wrinkles/folds, or 2D periodic array following laser interference patterns [28–32]. Some of these techniques are quite efficient to improve device performance but are very costly. Recently, Cho et al. has proposed textured plastic films attached to the external surface of the substrates of OSCs as spectrally neutral light trapping schemes [28]. In their study, they have demonstrated that random and V-groove texturing is very efficient to improve the performance of OSCs.

Thus, present study aims to simultaneously address issue of inefficient light absorption and inefficient charge collection. Thus, we have introduced an additional $PC_{70}BM$ layer to modify the interface between ZnO based electron transport layer (ETL) and photoactive layer. The photoactive layer comprised of Poly[4,8-bis(5-(2-ethylhexyl)thiophen-2-yl)benzo[1,2-b; 4,5-b′]dithiophene-2,6-diyl-alt-(4-(2-ethylhexyl)-3-fluorothieno[3,4-b]thiophene-)-2-carb-oxylate-2-6-diyl)] (PTB7-Th):$PC_{70}BM$. Devices were fabricated in an inverted geometry having a structure ITO/ZnO (40 nm)/$PC_{70}BM$ (5 nm)/PTB7-Th:$PC_{70}BM$ (100 nm)/MoO_3 (10 nm)/Ag (100 nm). Additionally, V-grooved textured PDMS films were attached to the backside of OSC substrates. Utilizing the interface modification and textured PDMS films, we have observed an increase in the power conversion efficiencies by ~37%. Our study suggests this performance enhancement after introduction of additional $PC_{70}BM$ layer between ZnO based ETL and photoactive layer is due to improved charge collection and observed improvement in OSCs with V-grooved textured PDMS films could be due to increased total optical path length.

2. Experimental

PTB7-Th (Lumtec), $PC_{70}BM$ (Lumtec, 99.5%), dichlorobenzene (DCB) (Aldrich, 99.9%), dichloromethane (Aldrich, 99.9%), MoO_3 (Alfa Aesar, 99.9995%), 1, 8 diiodooctane (DIO) and Silver (Alfa Aesar, 99.99%) were used as received without further purification.

2.1. Preparation of sol gel ZnO

Sol gel ZnO was prepared by the method reported elsewhere [14]. Briefly, 10 ml of 0.25M solution of Zinc acetate dihydrate (Aldrich, 99.9%) was prepared in 2-methoxy ethanol. Subsequently, 0.25M of ethanolamine was added to the solution and allowed to stir rigorously for 12 h at 70 °C to get a homogeneous, clear and transparent solution. Thereafter solution was aged for 24 h before using it for spin-coating as an electron transport layer.

2.2. Preparation of PDMS textured film

PDMS textured film was prepared by the method reported by Changsoon Cho et al. [28] Back-light enhancement films (BEF, Shinwha Intertek PTX338)used in the LCD industry were employed as masters. At first, PDMS(Sylgard 184, Dow Corning) base and cross linker were mixed in 10:1 wt ratio and allowed to stir for 30 min. This mixture was degassed for 30 min to remove the air bubbles. Textured PDMS films replicating the topology of the masters were then prepared by casting a pre-polymer (Sylgard 184, Dow Corning) on the masters and curing them at 90 °C for ~4 h.The textured PDMS films were peeled off, cleaned with isopropyl alcohol(IPA) to remove any dust particles and dried with nitrogen gun before attaching to the backside of OPV substrates.

2.3. Device fabrication

At first, photoactive blend comprised of PTB7-Th (10 mg) and $PC_{70}BM$ (15 mg) was prepared in 1 ml of DCB with 3% v/v of 1, 8 diiodooctane (DIO) solvent as an additive. The solution was allowed to stir at 70 °C in the dark for at least 12 h. For the device fabrication, ITO coated glass substrates (Luminescence Technology corp. Taiwan, with a sheet resistance of 15 Ωsq^{-1} and transmittance >85%) were cleaned by process reported elsewhere [14,15]. Thereafter, sol gel ZnO, which was previously synthesized, was spin-coated on pre-cleaned ITO substrates at 2000 rpm for 30 s to obtain a film of ~40 nm. The substrates were then annealed at 200 °C for 15min to remove excess solvents. Thereafter, substrates were transferred inside nitrogen filled glove box and a photoactive blend was spin-coated at 900 rpm for 120sec. The films were allowed to get dried for 2 h and then subsequently, the devices were evaporated using the shadow mask by thermal evaporation of 10 nm MoO_3layer as a hole transport layer and 100 nm Ag electrode as anode. For the devices with the additional $PC_{70}BM$ interlayer, $PC_{70}BM$ solution (10 mg/ml in DCM) was spin-coated on top of the ZnO nanocrystalline thin film at a speed of 1200 rpm for 60 s and annealed at 70 °C for 10min.The reason for selecting the DCM for making the $PC_{70}BM$ solution is because of its orthogonality with DCB. This is very important to avoid washing out or mixing of underneath $PC_{70}BM$ interlayer during the upper layer (photoactive layer) spin-coating.

2.4. Device characterization and testing

The current density-voltage (J-V) characteristics curves of fabricated devices with and without $PC_{70}BM$ interlayer and/or textured PDMS films were measured using a Keithley 2600 source meter and a Newport solar simulator (model number 91160) shines light with AM 1.5 G spectral distribution, which was calibrated using a certified reference solar cell to an intensity of 1000 W/m^2. The test cells were masked with a single aperture and care has been taken to exclude all light from entering the cell elsewhere, including shading of the edges of the substrates. The active device area is defined as 4.5 mm^2 by using a shadow mask. After measurement of the devices, a V-grooved textured PDMS films were attached to the backside of OSC substrates and measurements were taken again. Field Emission Gun-Scanning Electron Microscope (FEG-SEM) images were taken using JEOL JSM-7600F FEG-SEM instrument. The absorption studies were carried out using PerkinElmer Lambda 950 UV/VIS/NIR spectrophotometer.

2.5. Simulation studies

All simulations were performed using the finite element method (FEM) using commercially available COMSOL Multiphysics. Both Ray optics and wave mechanics module were studied. For geometric optics, surface is illuminated with 3 rays/release and general reflection wall condition is employed. For EM frequency domain, transverse magnetic wave in-plane vector was considered along with scattering boundary condition for inactive boundaries. The groove period and thickness of textured film was ~50 μm and ~25 μm respectively. For all simulation purpose, the refractive index was assumed to be constant and were considered as $RI_{PDMS} = 1.41$, $RI_{BS} = 1.517$ and $RI_{Air} = 1$.

3. Results and discussion

Fig. 1(a) depicts the SEM image of prepared V-groove textured PDMS film (inset: high magnification image highlighting the vertex angle). As can be seen, top part of the film consists of a V- groove array. The inter-groove array distance is ~50 μm and angle of vertex is around 100°. These physical specification as replicated on the PDMS film from the masters lies in the optimal range as reported in the previous studies and therefore absorption studies were carried out to verify whether PDMS textured film contributes towards the geometrical light trapping [28]. Fig. 1(b) shows normalised UV–Vis absorption spectra of photoactive blend films comprised of PTB7-Th:$PC_{70}BM$ with and without PDMS textured film. In both the cases, spectra of active layer comprised of two prominent peaks one corresponding to $PC_{70}BM$ at around 485 nm and other corresponding to PTB7-Th between 650 nm and 750 nm can be clearly observed [11]. However, for the active layer with the PDMS textured film, an enhancement in absorbance was observed over the broad spectral range. To understand the origin of this observed enhancement in absorbance for the active layer with the PDMS textured film in comparison to the active layer without PDMS textured film, an optical simulations were carried out using COMSOL multiphysics.

Fig. 2(a) and (b) demonstrates the ray optics simulations for the glass substrates with and without textured PDMS films respectively. The less number of incident rays and periodicity in the V-groove textured PDMS films offers an opportunity to trace the light path with more clarity. As can be observed clearly, incident ray undergo several scattering at the surface of the textured PDMS films and thereby increases the path length of the incident light within the active layer. However, to make these scattering more effective towards increasing the path length of the incident light within the active layer, an optimized vertex angle has to be employed. Previous studies have suggested that vertex angle between 90 and 115° is optimal for normal incidence and allows the maximum light trapping [28]. Thus, in the present study, a vertex angle of 100° is employed to achieve maximum trapping. For the glass substrates without textured PDMS films, incident light undergoes only transmission and reflection and there is hardly any scattering. Thus, in this arrangement path length of the incident light within the active layer is less when compared to the glass substrates with textured PDMS film. Fig. 2(c) and (d) illustrates the wave optics simulations for the glass substrates with and without textured PDMS films respectively. It can be clearly observed that more number of photons are available at the PDMS/glass interface which can be absorbed by the active layer. Thus both ray optics and wave mechanics simulations confirm that the presence of the textured PDMS films at the air/glass interface can increase the optical path length the of the incident light within the active layer due to geometrical light trapping and is consistent with the previous studies.

Taking into consideration absorption data and simulation studies, devices were fabricated with inverted geometry having a structure ITO/ZnO/$PC_{70}BM$/PTB7-Th:$PC_{70}BM$/MoO_3/Ag. It is worth mentioning here thin $PC_{70}BM$ interlayer has been introduced between ZnO based ETL and photoactive layer comprised of PTB7-Th:$PC_{70}BM$ so as to improve the charge collection and it has nothing to do with the light trapping. Fig. 3(a and b) shows the device architecture and energy band diagram respectively, of solar cells studied in this work [14,22,33]. As can be seen, a $PC_{70}BM$ interlayer is inserted between the ZnO based ETL and photoactive layer comprised of PTB7-Th:$PC_{70}BM$ and v-grooved textured PDMS film is applied on the backside of OSC substrates. Also, energy levels of the various materials used in the device fabrication are well aligned and therefore we hypothesize the efficient charge transfer.

At first, effect of the PDMS textured film on the control device (ITO/ZnO/PTB7-Th:$PC_{70}BM$/MoO_3/Ag.) was studied. Fig. 4(a) and (b) demonstrates a comparison of the current density–voltage (J–V) characteristics curves and external quantum efficiency (EQE) spectra for the control device with and without PDMS textured

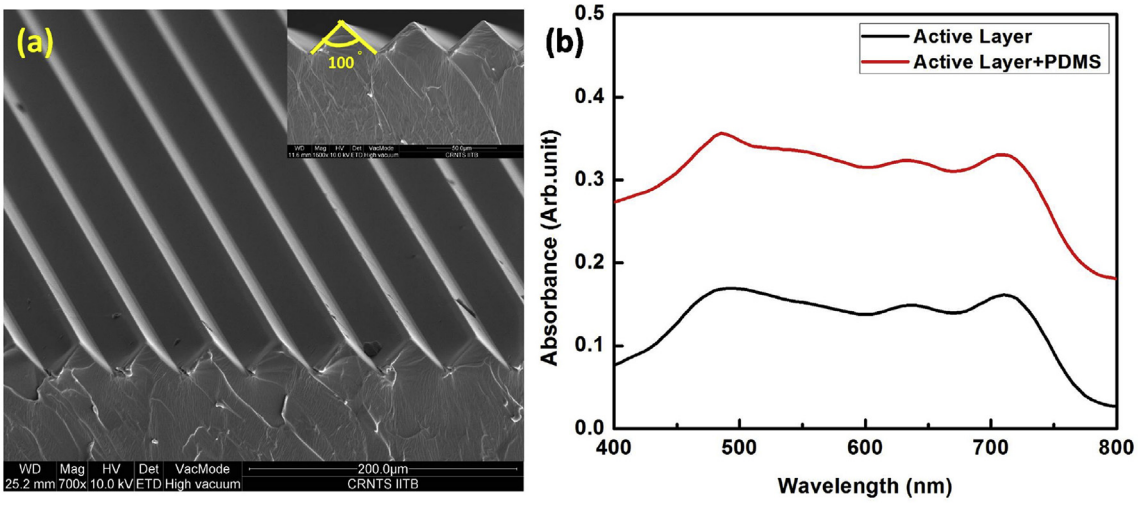

Fig. 1. (a) SEM image of V-groove textured PDMS film (inset: high magnification image highlighting the vertex angle) and (b) UV–Vis absorption spectra of photoactive blend films comprised of PTB7-Th:$PC_{70}BM$ with and without PDMS textured film.

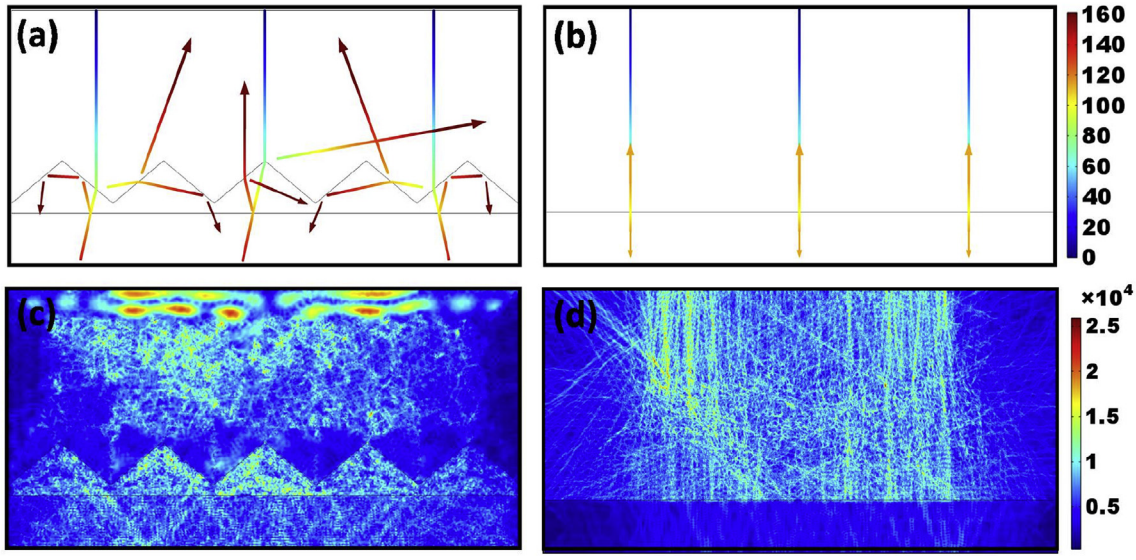

Fig. 2. (a)–(b) Ray optics simulations and (c)–(d) wave optics simulations for the glass substrates with and without textured PDMS films respectively.

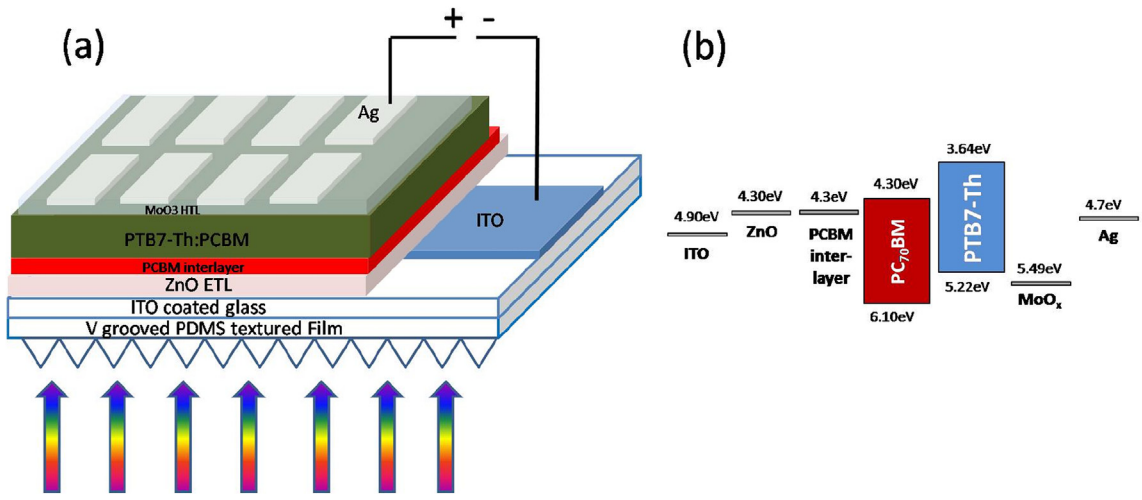

Fig. 3. (a) Schematic highlighting device architecture ITO/ZnO/$PC_{70}BM$/PTB7-Th:$PC_{70}BM$/MoO_3/Ag (b) Energy levels of materials used in the solar cell device.

films and various performance parameters such as open circuit voltage (Voc), short circuit current density (Jsc), fill factor (FF) and power conversion efficiency (PCE) of the above mentioned devices has been described in Table 1. As can be seen, for both the devices, the Voc and FF almost remains unchanged. However, when a V-grooved textured PDMS film was applied, a substantial increase of ~15% is observed in the Jsc and PCE. This influence on the cell operation was much anticipated as an optimized version of the V-grooved textured PDMS films can be attributed to the external light trapping configuration. Similar trend was observed during EQE spectra measurement of the devices with and without the V-groove textured film. Fig. 4(b) highlights that enhancement in EQE spectra was over the broad spectral range and is in conformity with the observed increase in the J-V characteristics spectra and absorption spectra shown in Fig. 1(b).

To elucidate the effect of the only $PC_{70}BM$ interlayer and overall effect of the $PC_{70}BM$ interlayer along with PDMS textured film, devices were fabricated having a structure ITO/ZnO/$PC_{70}BM$/PTB7-Th:$PC_{70}BM$/MoO_3/Ag. Fig. 4(c) and (d) demonstrates a comparison of the J–V characteristics curves and EQE spectra for the control device, devices having $PC_{70}BM$ interlayer with/without PDMS textured films. Various performance parameters of the above mentioned devices have been described in Table 1. Upon comparison for the devices with and without $PC_{70}BM$ interlayer between ZnO based ETL and photoactive layer, it was found that both Jsc and FF increases considerably and as a result PCE increases from 6.65 to 7.74%. This is in agreement with the previous reports and can be attributed to the quenching of the electron–hole recombination at the interface of ZnO based ETL and the photoactive layer [25]. However, when a V- grooved textured PDMS film was applied to the devices having $PC_{70}BM$ interlayer, an additional increase of ~18% was observed in the Jsc. As a result PCE further increases from 7.74 to 9.12%. Similar trend was observed during EQE spectra measurement of the above mentioned devices and has been highlighted in the Fig. 4(d).

To explain the improvement in performance parameter for the devices with the $PC_{70}BM$ interlayer between ZnO based ETL and photoactive layer, surface morphological studies of the polymer blend films were characterized by atomic force microscopy (AFM). Fig. 5(a)–(d) demonstrates AFM images of films of ZnO, active layer

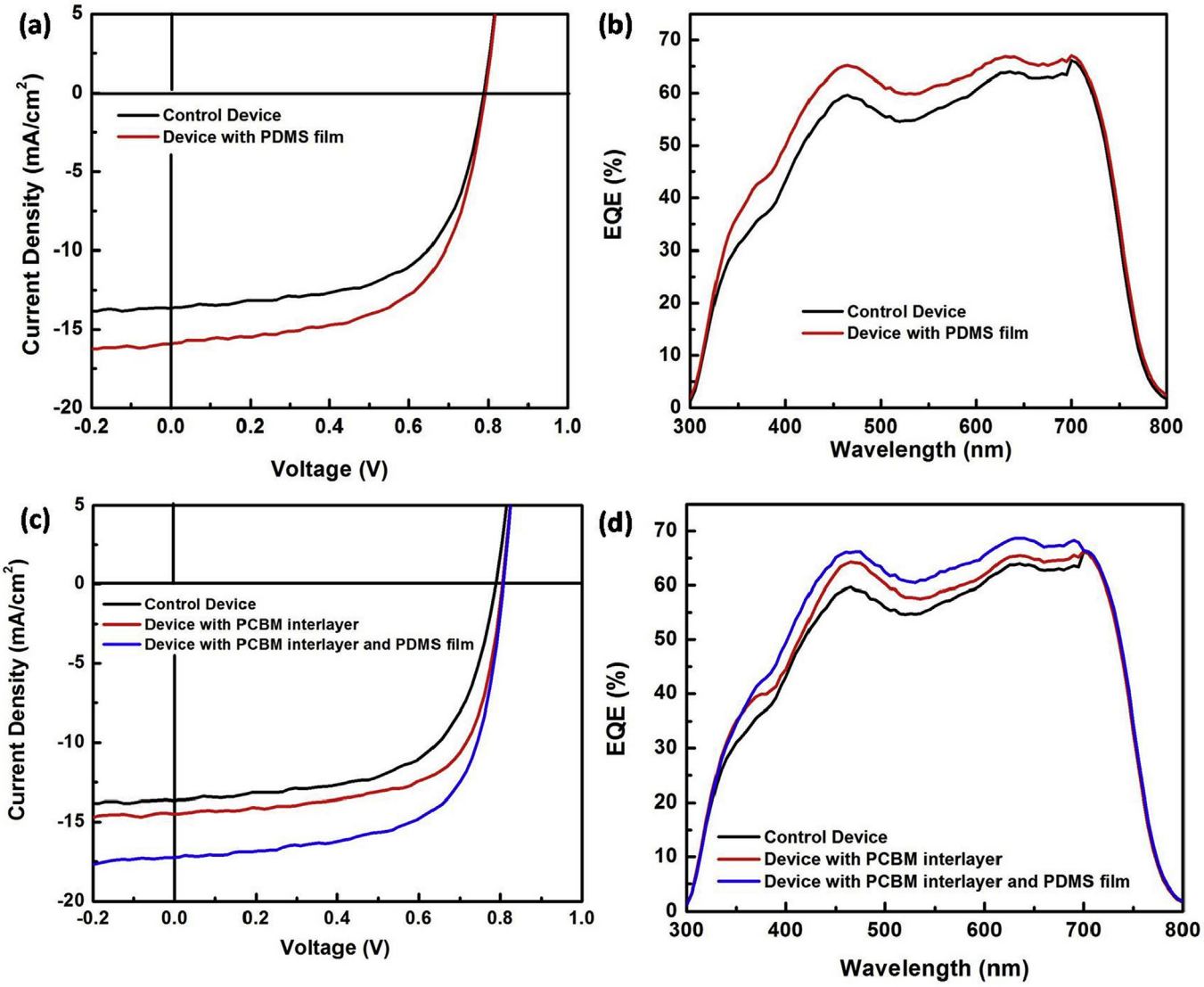

Fig. 4. (a,c) *J-V* characteristics under illumination (AM 1.5G, 1 sun) and (b,d) EQE spectra of fabricated devices.

Table 1
Performance parameters for fabricated devices with various device architectures.

Device architecture		V_{oc} (V)	J_{sc} (mA/cm^2)	FF (%)	PCE[a] (%)
Control Device	Without PDMS	0.79	13.80	61.06	6.65 (6.57)
	With PDMS	0.79	15.91	61.79	7.77 (7.69)
Device with $PC_{70}BM$ interlayer	Without PDMS	0.80	14.51	66.18	7.74 (7.62)
	With PDMS	0.80	17.27	65.62	9.12 (8.59)

[a] The average PCE is shown in parentheses. Average PCE was calculated using the results of 5 devices.

deposited on ZnO, $PC_{70}BM$ and active layer deposited on PCBM/ZnO respectively. As can be observed, the active layer film deposited on ZnO has surface roughness of 3.98 nm. However, this surface roughness gets reduced to 1.53 nm when the active layer film is deposited on $PC_{70}BM$/ZnO. Thus, it can be concluded that introduction of $PC_{70}BM$ interlayer between ZnO based ETL and photoactive layer helps in achieving the improved quality of the interfaces. This is in consistence with the previous studies which demands films with less surface roughness to achieve improved device performance [24,25]. To explain the improved performance, studies evinced that smoother film facilitates the uniform active layer deposition, which in turn decreases the interfacial series resistance. We believe it is this interface engineering which has quenched the electron–hole recombination at the interface and has improved power conversion efficiency (PCE) from 6.65 to 7.74%.

4. Conclusion

In conclusion, we have successfully made a V-grooved textured PDMS film and applied it on the backside of OSC substrates along

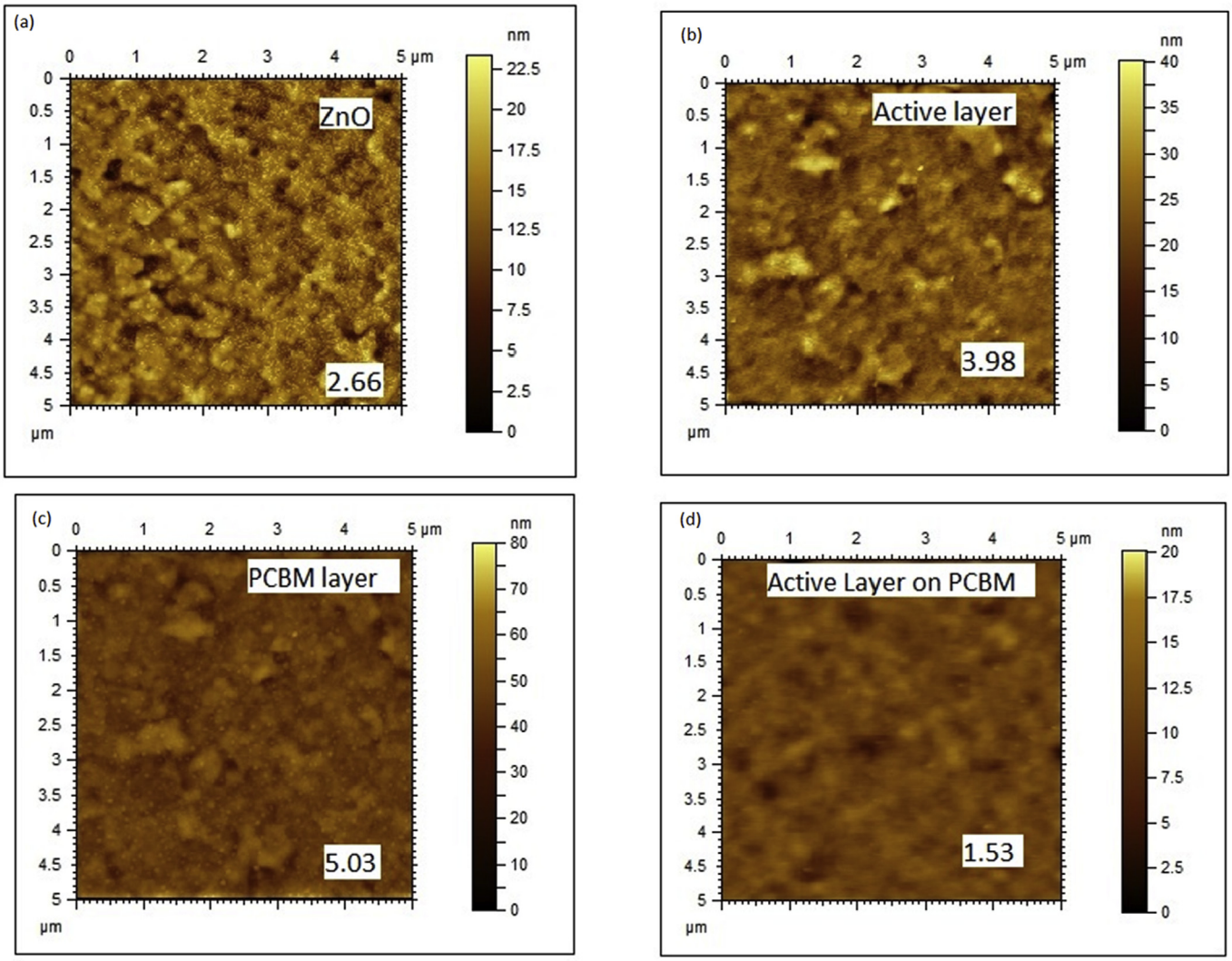

Fig. 5. Atomic Force Microscopy (AFM) images of (a) ZnO, (b) active layer deposited on ZnO, (c) $PC_{70}BM$ and (d) active layer deposited $PC_{70}BM$/ZnO respectively.

with an introduction of $PC_{70}BM$ interlayer between ZnO based ETL and photoactive layer. Our study confirms that use of the $PC_{70}BM$ interlayer improves Jsc and FF. The possible reasons for the increase in the FF and Jsc for the devices with $PC_{70}BM$ interlayer and Jsc for the devices with V-grooved textured PDMS film was also discussed. We believe the results from the present study will provide critical strategy for simultaneously improving the charge collection and photon absorption to demonstrate fabrication of high-efficiency organic solar cells.

Acknowledgments

The authors would like to acknowledge the support of Center of Excellence in Nanoelectronics (CEN), National Center for Photovoltaic Research and Education (NCPRE), Department of Metallurgical Engineering and Materials Science (MEMS) and Sophisticated Analytical Instrument Facility (SAIF) at Indian Institute of Technology Bombay (IIT Bombay) Mumbai for providing various facilities for device fabrication and characterization. A.Y. thanks the DST-INSPIRE fellowship for the financial support. We also thank for partial support under the Solar Energy Research Institute for India and the United States (SERIIUS), funded jointly by the U.S. Department of Energy (Office of Science, Office of Basic Energy Sciences, and Energy Efficiency and Renewable Energy, Solar Energy Technology Program, under Subcontract DE-AC36-08GO28308 to the National Renewable Energy Laboratory, Golden, Colorado) and the Government of India, through the Department of Science and Technology under Subcontract IUSSTF/JCERDC-SERIIUS/2012 dated 22nd Nov. 2012.

References

[1] T.M. Clarke, J.R. Durrant, Charge photogeneration in organic solar cells, Chem. Rev. 110 (2010) 6736–6767.
[2] Y. Kim, S. Cook, S.M. Tuladhar, S.A. Choulis, J. Nelson, J.R. Durrant, D.D.C. Bradley, M. Giles, I. Mcculloch, C.S. Ha, M. Ree, A strong regioregularity effect in self-organizing conjugated polymer films and high-efficiency polythiophene: fullerene solar cells, Nat. Mater. 5 (2006) 197–203.
[3] S. Gunes, H. Neugebauer, N.S. Sariciftci, Conjugated polymer-based organic solar cells, Chem. Rev. 107 (2007) 1324–1338.
[4] G. Yu, J. Gao, J.C. Hummelen, F. Wudl, A.J. Heeger, Polymer photovoltaic cells - enhanced efficiencies via a network of internal donor-acceptor heterojunctions, Science 270 (1995) 1789–1791.
[5] M.C. Scharber, D. Wuhlbacher, M. Koppe, P. Denk, C. Waldauf, A.J. Heeger, C.L. Brabec, Design rules for donors in bulk-heterojunction solar cells - towards 10 % energy-conversion efficiency, Adv. Mater. 18 (2006) 789–794.
[6] J.B. You, L. Meng, T.B. Song, T.F. Guo, Y. Yang, W.H. Chang, Z.R. Hong, H.J. Chen, H.P. Zhou, Q. Chen, Y.S. Liu, N. De Marco, Y. Yang, Improved air stability of

perovskite solar cells via solution-processed metal oxide transport layers, Nat. Nanotechnol. 11 (2016) 75–81.
[7] N.G. Park, Perovskite solar cells: an emerging photovoltaic technology, Mater. Today 18 (2015) 65–72.
[8] Y. Zang, C.Z. Li, C.C. Chueh, S.T. Williams, W. Jiang, Z.H. Wang, J.S. Yu, A.K.Y. Jen, Integrated molecular, interfacial, and device engineering towards high-performance non-fullerene based organic solar cells, Adv. Mater. 26 (2014) 5708–5714.
[9] G.J. Zhao, Y.J. He, Y.F. Li, 6.5% efficiency of polymer solar cells based on poly(3-hexylthiophene) and Indene-C-60 bisadduct by device optimization, Adv. Mater. 22 (2010) 4355–4358.
[10] Y.J. He, H.Y. Chen, J.H. Hou, Y.F. Li, Indene-C-60 bisadduct: a new acceptor for high-performance polymer solar cells, J. Am. Chem. Soc. 132 (2010) 1377–1382.
[11] Z.C. He, B. Xiao, F. Liu, H.B. Wu, Y.L. Yang, S. Xiao, C. Wang, T.P. Russell, Y. Cao, Single-junction polymer solar cells with high efficiency and photovoltage, Nat. Photonics 9 (2015) 174–179.
[12] Y.H. Liu, J.B. Zhao, Z.K. Li, C. Mu, W. Ma, H.W. Hu, K. Jiang, H.R. Lin, H. Ade, H. Yan, Aggregation and morphology control enables multiple cases of high-efficiency polymer solar cells, Nat. Commun. 5 (2014) 1–8.
[13] W.L. Ma, C.Y. Yang, X. Gong, K. Lee, A.J. Heeger, Thermally stable, efficient polymer solar cells with nanoscale control of the interpenetrating network morphology, Adv. Funct. Mater. 15 (2005) 1617–1622.
[14] R. Sharma, S. Bhalerao, D. Gupta, Effect of incorporation of CdS NPs on performance of PTB7: PCBM organic solar cells, Org. Electron 33 (2016) 274–280.
[15] R. Sharma, H. Lee, V. Gupta, H. Kim, M. Kumar, C. Sharma, S. Chand, S. Yoo, D. Gupta, Photo-physics of PTB7, PCBM and ICBA based ternary solar cells, Org. Electron 34 (2016) 111–117.
[16] S.H. Park, A. Roy, S. Beaupre, S. Cho, N. Coates, J.S. Moon, D. Moses, M. Leclerc, K. Lee, A.J. Heeger, Bulk heterojunction solar cells with internal quantum efficiency approaching 100%, Nat. Photonics 3 (2009) 297–302.
[17] S. Kundu, S.R. Gollu, R. Sharma, G. Srinivas, A. Ashok, A.R. Kulkarni, D. Gupta, Device stability of inverted and conventional bulk heterojunction solar cells with MoO3 and ZnO nanoparticles as charge transport layers, Org. Electron 14 (2013) 3083–3088.
[18] S.R. Gollu, R. Sharma, G. Srinivas, S. Kundu, D. Gupta, Incorporation of silver and gold nanostructures for performance improvement in P3HT: PCBM inverted solar cell with rGO/ZnO nanocomposite as an electron transport layer, Org. Electron 29 (2016) 79–87.
[19] S.R. Gollu, R. Sharma, G. Srinivas, S. Kundu, D. Gupta, Incorporation of SiO2 dielectric nanoparticles for performance enhancement in P3HT: PCBM inverted organic solar cells, Org. Electron 24 (2015) 43–50.
[20] S.R. Gollu, R. Sharma, G. Srinivas, S. Kundu, D. Gupta, Effects of incorporation of copper sulfide nanocrystals on the performance of P3HT: PCBM based inverted solar cells, Org. Electron 15 (2014) 2518–2525.
[21] J.Y. Kim, S.H. Kim, H.H. Lee, K. Lee, W.L. Ma, X. Gong, A.J. Heeger, New architecture for high-efficiency polymer photovoltaic cells using solution-based titanium oxide as an optical spacer, Adv. Mater. 18 (2006) 572–576.
[22] S.H. Liao, H.J. Jhuo, Y.S. Cheng, S.A. Chen, Fullerene derivative-doped Zinc oxide nanofilm as the cathode of inverted polymer solar cells with low-bandgap polymer (PTB7-Th) for high performance, Adv. Mater. 25 (2013) 4766–4771.
[23] D. Yang, P. Fu, F.J. Zhang, N. Wang, J. Zhang, C. Li, High efficiency inverted polymer solar cells with room-temperature titanium oxide/polyethylenimine films as electron transport layers, J. Mater. Chem. A 2 (2014) 17281–17285.
[24] S. Woo, W.H. Kim, H. Kim, Y. Yi, H.K. Lyu, Y. Kim, 8.9% single-stack inverted polymer solar cells with electron-rich polymer nanolayer-modified inorganic electron-collecting buffer layers, Adv. Energy Mater. 4 (1301692) (2014) 1–7.
[25] S. Cho, K.D. Kim, J. Heo, J.Y. Lee, G. Cha, B.Y. Seo, Y.D. Kim, Y.S. Kim, S.Y. Choi, D.C. Lim, Role of additional PCBM layer between ZnO and photoactive layers in inverted bulk-heterojunction solar cells, Sci. Rep-UK 4 (4306) (2014) 1–6.
[26] K. Topp, H. Borchert, F. Johnen, A.V. Tune, M. Knipper, E. von Hauff, J. Parisi, K. Al-Shamery, Impact of the incorporation of Au nanoparticles into polymer/fullerene solar cells, J. Phys. Chem. A 114 (2010) 3981–3989.
[27] L.Y. Lu, Z.Q. Luo, T. Xu, L.P. Yu, Cooperative plasmonic effect of Ag and Au nanoparticles on enhancing performance of polymer solar cells, Nano Lett. 13 (2013) 59–64.
[28] C. Cho, H. Kim, S. Jeong, S.W. Baek, J.W. Seo, D. Han, K. Kim, Y. Park, S. Yoo, J.Y. Lee, Random and V-groove texturing for efficient light trapping in organic photovoltaic cells, Sol. Energ Mat. Sol. C 115 (2013) 36–41.
[29] M. Niggemann, M. Glatthaar, P. Lewer, C. Muller, J. Wagner, A. Gombert, Functional microprism substrate for organic solar cells, Thin Solid Films 511 (2006) 628–633.
[30] M. Niggemann, M. Glatthaar, A. Gombert, A. Hinsch, V. Wittwer, Diffraction gratings and buried nano-electrodes - architectures for organic solar cells, Thin Solid Films 451 (2004) 619–623.
[31] J.B. Kim, P. Kim, N.C. Pegard, S.J. Oh, C.R. Kagan, J.W. Fleischer, H.A. Stone, Y.L. Loo, Wrinkles and deep folds as photonic structures in photovoltaics, Nat. Photonics 6 (2012) 327–332.
[32] L. Muller-Meskamp, Y.H. Kim, T. Roch, S. Hofmann, R. Scholz, S. Eckardt, K. Leo, A.F. Lasagni, Efficiency enhancement of organic solar cells by fabricating periodic surface textures using direct laser interference patterning, Adv. Mater. 24 (2012) 906–910.
[33] S.H. Liao, H.J. Jhuo, P.N. Yeh, Y.S. Cheng, Y.L. Li, Y.H. Lee, S. Sharma, S.A. Chen, Single junction inverted polymer solar cell reaching power conversion efficiency 10.31% by employing dual-doped Zinc oxide nano-film as cathode interlayer, Sci. Rep-UK 4 (6813) (2014) 1–7.